

Supplementary Information

X-ray Fluorescence Imaging of the Hippocampal Formation after Manganese Exposure[†]

Gregory Robison^a, Taisiya Zakharova^a, Sherleen Fu^b, Wendy Jiang^b, Rachael Fulper^a, Raul Barrea^{c,d}, Wei Zheng^b, Yulia Pushkar^{*a}

^a Purdue University, Department of Physics, 525 Northwestern Avenue, West Lafayette, IN 47907, USA. Fax: (765)494-0706; Tel: (765)496-3276
E-mail: ypushkar@purdue.edu

^b Purdue University, School of Health Sciences, 550 Stadium Mall Drive, West Lafayette, IN 47907, USA.

^c DePaul University, Department of Physics, 2219 North Kenmore Avenue Suite 211, Chicago, IL 60614, USA.

^d Argonne National Laboratory, Advanced Photon Source, 9700 South Cass Avenue, Argonne, IL 60437, USA (former affiliation)

Table of Contents

Table of Contents.....	1
Methods	2
Glial fibrillary acidic protein immunohistochemistry.....	2
Detection and analyzable limits	2
Figures.....	4
Fig. S1: HPCf cell scan locations.....	4
Fig. S2: HPCf CA3 Control cells.....	5
Fig. S3: HPCf CA3 Mn Treated cells	6
Fig. S4: HPCf 1-5 pixel scatter plots	7
Fig. S5: Pixel scatter plots of CA3 cells	8
Fig. S6: Glial fibrillary acidic protein immunohistochemical staining of the HPCf.....	9
Tables	10
Table S1: Minimum detection and analyzable limits.....	10
Table S2: Linear fit parameters for HPCf pixel scatter plots	11
Abbreviation	12
References.....	12

Methods

Glial fibrillary acidic protein immunohistochemistry

Glial fibrillary acidic protein serves as a marker of astrocytes. Ten micron thick sections stored at -80°C were thawed and fixed with 4% paraformaldehyde in phosphate buffered saline (PBS; 137mM sodium chloride, 2.7mM potassium chloride, 10mM disodium phosphate, and 1.8mM monopotassium phosphate; pH 7.4) for 10 minutes at room temperature. Following fixation, samples were washed three times with PBS (5 minutes per wash) and treated at room temperature sequentially with: 1) blocking/permeabilization solution: (2% bovine serum albumin (BSA) / 0.2% (w/v) Triton X-100 in PBS) for 1 hour, 2) mouse anti-glial fibrillary acidic protein (Millipore AB360) contained in PBS containing 2% BSA at 1:400 dilution for 2 hours, and 3) secondary Alexa Fluor 488 goat anti-mouse IgG antibodies in PBS containing 2% BSA at 1:1000 dilution for 1 hour. Three washes with PBS (5 minutes per wash) were performed after treatment with primary and secondary antibodies. Upon completion, ProLong Gold antifade reagent was applied to each section, the sections covered, and sealed. Images were taken acquired using an Eclipse TE2000-U inverted microscope outfitted with an Eclipse C1 Plus confocal system (Nikon Instruments Inc.). NIS-Elements BR 3.0 software was used to capture the images and FIJI software used to stitch images.

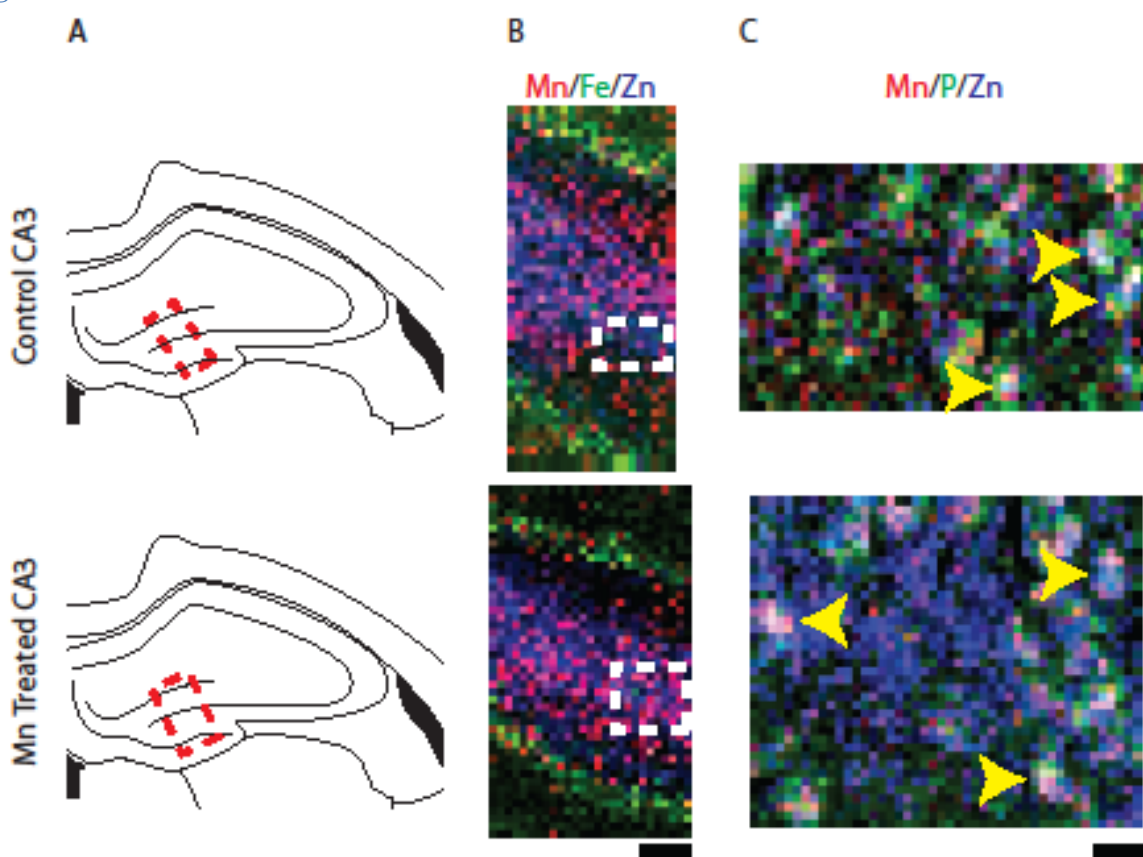
Detection and analyzable limits

Minimum detection limits (MDL) and minimum analyzable limits (MAL) were approximated using spectra of NIST standards (formerly NBS 1832/1833¹). Briefly, the user defined the range containing a signal for a desired element (e.g. Mn) and the peak was identified according to maximum counts within this range. The endpoints of the range were used to approximate the background using a linear fit. Next, the distances from the peak location to the lower and upper bounds of the range were determined and the lower of these two values selected to create a new

symmetric range about the peak (henceforth referred to as the signal window). Using the signal window, the total counts were calculated from the spectrum and the background counts were determined using the linear background approximation. The signal window was then narrowed by two channels and the process repeated until the signal window was only 2 channels wide. The maximum signal to background ratio was selected for calculating the MDL and MAL²⁻³. For the MDL calculations, a 95% confidence threshold was used to determine the presence of a signal (i.e. signal must be 1.654 sigma above the background). For the MAL calculations, a signal 10 sigma above the background was deemed sufficient. Results are given in Table S1.

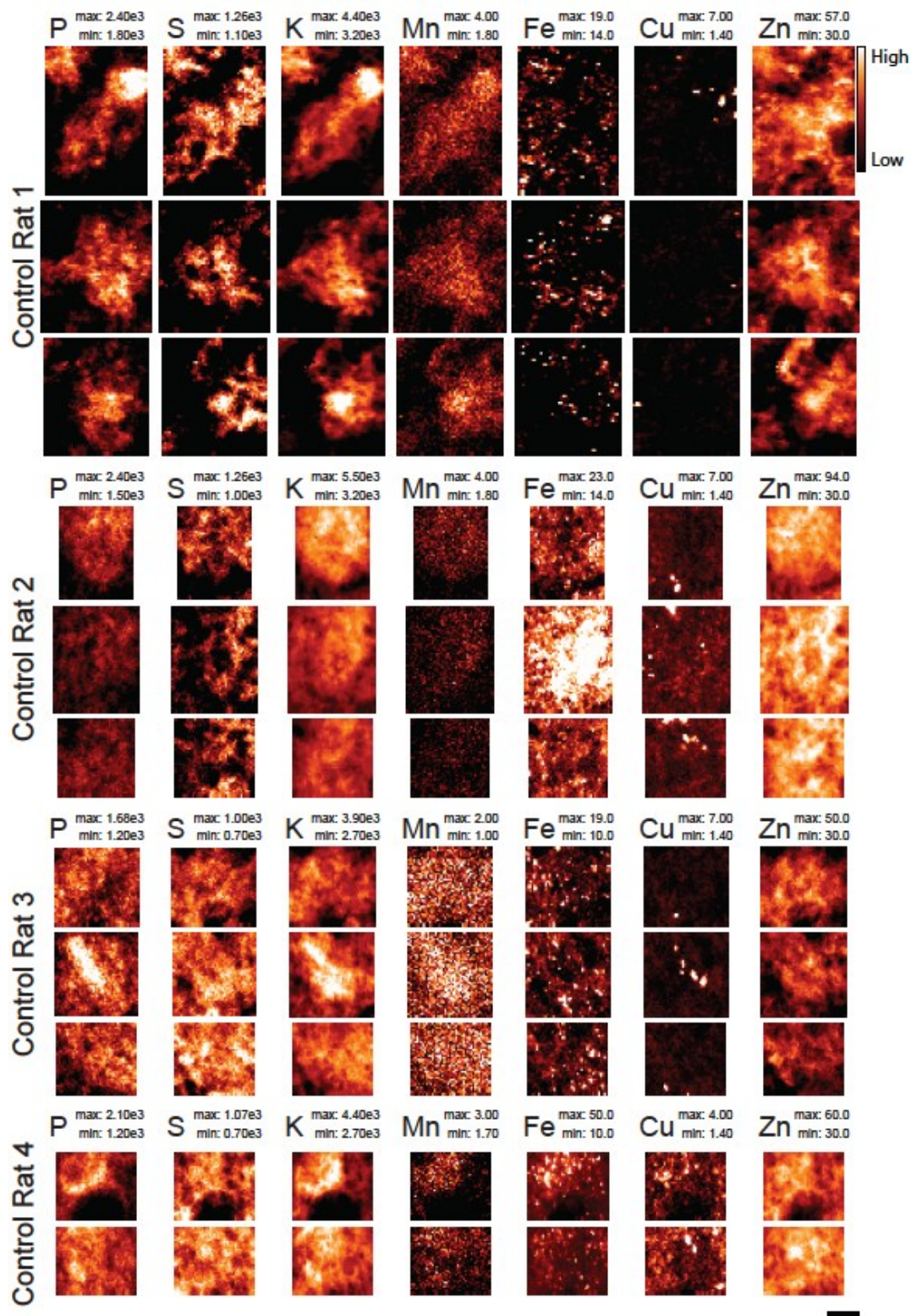
Figures

Fig. S1: HPCf cell scan locations



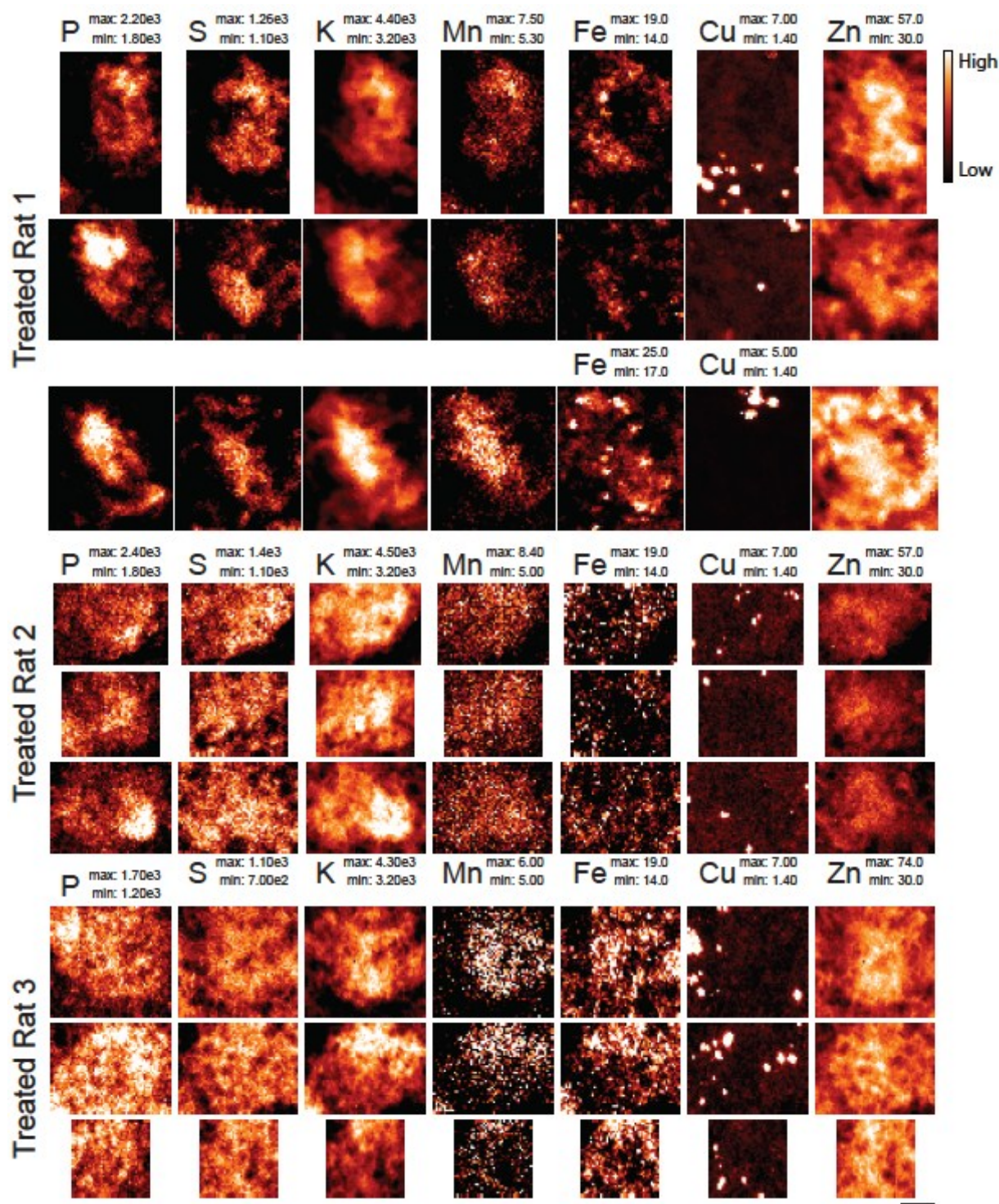
(A) Diagram of the HPCf at Bregma -2.64mm. The dashed red box indicates the approximate region for XRF images ($\sim 15\mu\text{m} \times 15\mu\text{m}$ resolution) as displayed in (B). White dashed boxes in (B) indicated the approximate region of XRF images ($3\mu\text{m} \times 3\mu\text{m}$ resolution) as shown in (C). Yellow arrowheads in (C) indicate several cells selected for subcellular resolution XRF imaging ($0.3\mu\text{m} \times 0.3\mu\text{m}$ resolution). Cells were selected based on their phosphorus and zinc signal, the latter to ensure that the cell was in Ammon's horn of the HPCf. Scale bar represents a length of $100\mu\text{m}$ (B) and $20\mu\text{m}$ (C).

Fig. S2: HPCf CA3 Control cells



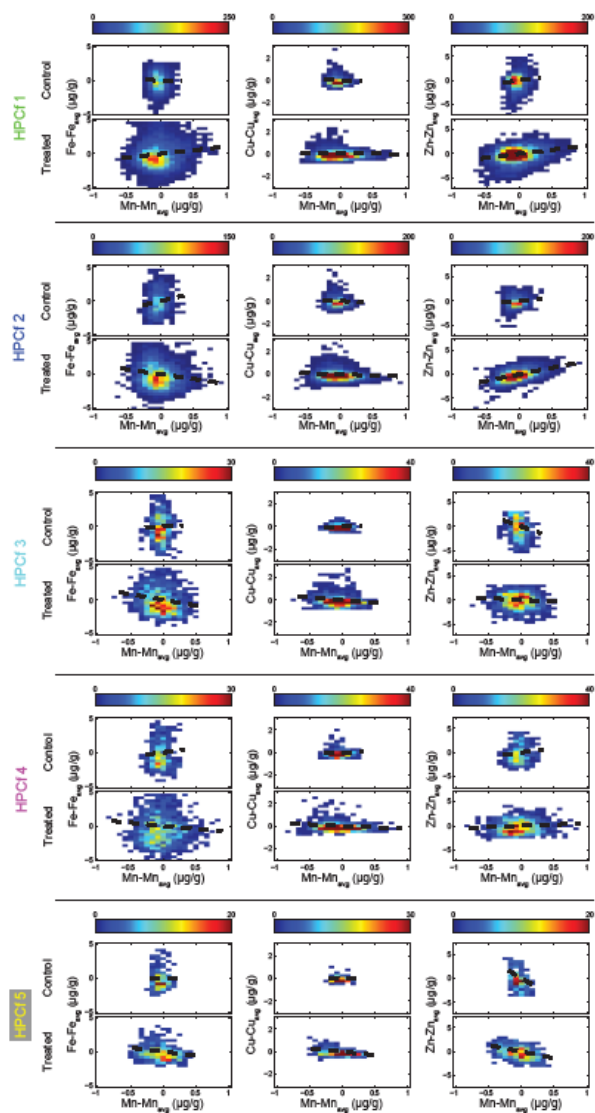
XRF images of cells from control samples. Note different color scale values for a given animal. Given values are in µg/g. Scale bar represents a length of 5µm.

Fig. S3: HPCf CA3 Mn Treated cells



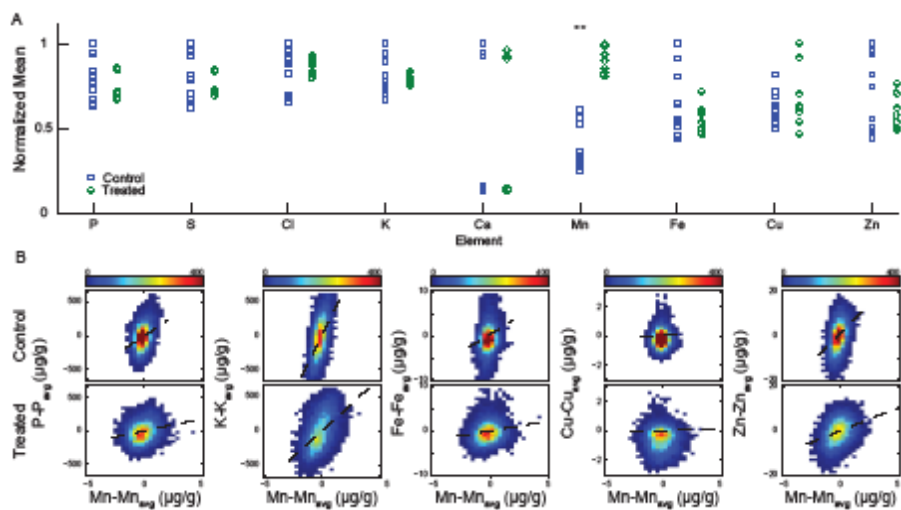
XRF images of cells from treated samples. Note different color scale values for a given animal. Given values are in $\mu\text{g/g}$. Scale bar represents a length of $5\mu\text{m}$.

Fig. S4: HPCf 1-5 pixel scatter plots



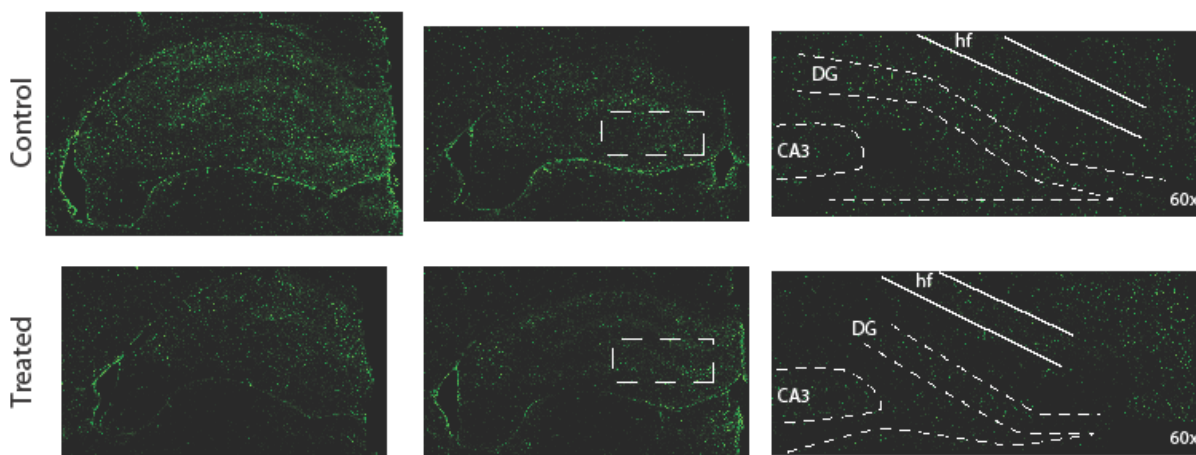
Binned scatter plots of pixel values for the regions of the hippocampus as identified by k-means cluster analysis. The average metal content for a given region was subtracted from each pixel value contained within that region. Pixel data for all control (top) or treated (bottom) samples were then combined and binned to form two-dimensional histograms where the color scale indicates the number of pixels contributing to a given bin. Black dashed lines display the linear regression fit for the un-binned data; fit parameters and ANCOVA results are given in Table S2.

Fig. S5: Pixel scatter plots of CA3 cells



(A) Scatter plot showing the average metal content for all imaged cells ($n=11/9$, control/treated). Average metal concentration was determined for each cell and then normalized by the maximum concentration measured for the given metal. Note that there is up to 40% variation in metal concentration. For a portion of the data, Ca was below the analyzable limit, explaining the bi-modal distribution of values. Mn was the only metal that demonstrated a statistically significant difference in content (** $p < 0.01$). **(B)** Pixel scatter plot of control (top) and Mn treated (bottom) cells. For a given cell, the cell body was delineated using the potassium signal as outlined in Experimental Procedures section. Black dashed lines display the linear regression fit for the un-binned data; fit parameters and ANCOVA results are given in Table 6.

Fig. S6: Glial fibrillary acidic protein immunohistochemical staining of the HPCf



Results of GFAP staining of control (top) and Mn treated (bottom) sections. The rightmost panel displays images taken at $\times 60$ of the crest of the DG; white dashed lines are included to assist with identification of various sub-structures. Staining is the strongest along the hf and CA1, followed by the DG and CA3.

Tables

Table S1: Minimum detection and analyzable limits

	Element	C _{std} (µg/cm ²)	Total (counts)	Background (counts)	Signal (counts)	C _{MDL} (µg/g)	C _{MAL} (µg/g)
APS Sector 18 Run 1	Mn	4.22	3.05E+03	4.36E+01	3.00E+03	1.61E+00	1.10E+01
	Fe	14.15	8.96E+03	4.50E+01	8.91E+03	1.85E+00	1.26E+01
	Cu	2.25	3.05E+03	9.04E+01	2.96E+03	1.25E+00	8.27E+00
	Zn	3.98	4.35E+03	4.56E+01	4.30E+03	1.08E+00	7.40E+00
APS Sector 18 Run 2	Mn	4.22	3.45E+05	3.02E+03	3.42E+05	1.67E-02	1.01E-01
	Fe	14.15	1.71E+05	7.74E+02	1.70E+05	5.67E-02	3.46E-01
	Cu	2.25	6.02E+05	1.33E+04	5.89E+05	1.08E-02	6.57E-02
	Zn	3.98	1.44E+05	1.07E+03	1.43E+05	2.23E-02	1.36E-01
APS Sector 2-ID-D Run 1	Mn	4.22	3.97E+05	4.60E+03	3.93E+05	1.79E-01	1.10E+00
	Fe	14.15	1.34E+06	8.09E+03	1.34E+06	2.34E-01	1.44E+00
	Cu	2.25	4.10E+05	8.89E+03	4.01E+05	1.30E-01	7.99E-01
	Zn	3.98	7.46E+05	7.76E+03	7.39E+05	1.16E-01	7.17E-01
APS Sector 2-ID-D Run 2	K	17.09	1.90E+05	1.56E+04	1.75E+05	4.04E+00	2.49E+01
	Mn	4.22	2.33E+05	2.58E+03	2.30E+05	3.08E-01	1.93E+00
	Fe	14.15	1.03E+06	6.61E+03	1.02E+06	3.73E-01	2.31E+00
	Cu	2.25	2.55E+05	4.57E+03	2.50E+05	2.01E-01	1.25E+00
	Zn	3.98	5.61E+05	4.44E+03	5.56E+05	1.58E-01	9.80E-01

Table S2: Linear fit parameters for HPCf pixel scatter plots

			Slope	<i>r</i>	<i>p</i>	<i>F</i>	<i>p</i>	<i>F</i>	<i>P</i>
Fe/Mn	Control	HPCf 1	-0.23 ± 0.28	-0.02	0.42			5.33 ^a	<0.01
		HPCf 2	2.25 ± 0.42	0.14	<0.01				
		HPCf 3	0.24 ± 0.90	0.01	0.79				
		HPCf 4	1.09 ± 0.87	0.05	0.21				
		HPCf 5	-0.04 ± 0.98	0	0.97				
	Treated	HPCf 1	1.07 ± 0.10	0.12	<0.01	9.28	<0.01	68.25 ^b	<0.01
		HPCf 2	-1.42 ± 0.13	-0.14	<0.01	53.20	<0.01		
		HPCf 3	-1.70 ± 0.26	-0.18	<0.01	5.06	0.02		
		HPCf 4	-0.92 ± 0.32	-0.08	<0.01	3.41	0.07		
		HPCf 5	-1.19 ± 0.25	-0.22	<0.01	1.72	0.19		
Cu/Mn	Control	HPCf 1	-0.19 ± 0.09	-0.04	0.04			2.82 ^c	0.02
		HPCf 2	-0.33 ± 0.11	-0.08	<0.01				
		HPCf 3	0.12 ± 0.08	0.06	0.14				
		HPCf 4	0.17 ± 0.13	0.06	0.19				
		HPCf 5	-0.27 ± 0.15	-0.11	0.08				
	Treated	HPCf 1	-0.01 ± 0.02	-0.01	0.56	3.83	0.05	24.04 ^{b,d}	<0.01
		HPCf 2	-0.21 ± 0.30	-0.09	<0.01	0.98	0.32		
		HPCf 3	-0.42 ± 0.07	-0.17	<0.01	8.92	<0.01		
		HPCf 4	-0.26 ± 0.05	-0.14	<0.01	6.08	0.01		
		HPCf 5	-0.60 ± 0.06	-0.41	<0.01	3.30	0.07		
Zn/Mn	Control	HPCf 1	2.08 ± 0.36	0.12	<0.01			37.86 ^e	<0.01
		HPCf 2	1.11 ± 0.29	0.10	<0.01				
		HPCf 3	-4.69 ± 0.85	-0.20	<0.01				
		HPCf 4	1.84 ± 0.74	0.11	0.01				
		HPCf 5	-8.06 ± 1.17	-0.38	<0.01				
	Treated	HPCf 1	1.65 ± 0.07	0.26	<0.01	1.81	0.18	159.82 ^f	<0.01
		HPCf 2	2.70 ± 0.07	0.49	<0.01	35.74	<0.01		
		HPCf 3	-0.68 ± 0.21	-0.09	<0.01	28.10	<0.01		
		HPCf 4	0.52 ± 0.15	0.10	<0.01	4.65	0.03		
		HPCf 5	-2.68 ± 0.26	-0.42	<0.01	28.85	<0.01		

^aHPCf2 slope differs from HPCf1

^bHPCf1 slope differs from all other regions

^cHPCf4 slope differs from HPCf2

^dHPCf2, 3, & 4 slopes differ from HPCf5

^eHPCf1, 2, & 4 slopes differ from HPCf3 & 5

^fAll HPCf region slopes differ from one another

ANCOVA results are compared to control slope of the same region.

Abbreviation

BSA	Bovine serum albumin
MAL	Minimum analyzable limit
MDL	Minimum detection limit
PBS	Phosphate buffered saline

References

1. P. A. Pella, D. E. Newbury, E. B. Steel, D. H. Blackburn, Development of National Bureau of Standards thin glass films for x-ray fluorescence spectrometry. *Anal. Chem.* 1986, **58**, 1133-1137.
2. B. S. Twining, S. B. Baines, N. S. Fisher, J. Maser, S. Vogt, C. Jacobsen, A. Tovar-Sanchez, S. A. Sanudo-Wilhelmy, Quantifying trace elements in individual aquatic protist cells with a synchrotron X-ray fluorescence microprobe. *Anal. Chem.* 2003, **75**, 3806-3816.
3. R. Jenkins, R. W. Gould, D. Gedcke, *Quantitative X-ray Spectrometry*. 2nd ed.; Marcel Dekker, Inc.: 1995; p 484.